Relationship between Brain Metabolism and Injury in Post-Cardiac Arrest Comatose Patients

Kevin Jia-Chen Chen

A thesis

submitted in partial fulfillment of the

requirements for the degree of

Master of Science

University of Washington

2024

Committee:

Mark Whipple

Edilberto Amorim de Cerqueira Filho

John Gennari

Program Authorized to Offer Degree:

Biomedical Informatics and Medical Education

University of Washington

Abstract

Relationship between Brain Metabolism and Injury in Post-Cardiac Arrest Comatose Patients

Kevin Jia-Chen Chen

Chair of the Supervisory Committee:
Mark Whipple
Biomedical Informatics and Medical Education

Cardiac arrest is a leading cause of death in the United States contributing to 5.6% of annual deaths. More than 80% of survivors are in permanent coma and 50-80% of those will die. Despite advancements in cardiac care, the mechanisms underlying brain injury are complex and not well understood, which has limited advancement in brain targeted therapies. Specifically, the relationship between regional brain metabolism and risk of brain injury is not known. This thesis investigated the relationship between brain injury in post-cardiac arrest comatose patients and metabolic characteristics: cerebral blood flow (CBF), cerebral blood volume (CBV), cerebral metabolic rate of oxygen ($CMRO_2$), and cerebral metabolic rate of glucose (CMR_{glu}) in healthy normal brains. The study analyzed whole brains, brains clustered by injury percentages, and brain regions clustered by injury percentage. Resulting correlations showed that $CMRO_2$ and CMR_{glu} had stronger correlations with brain injury than CBF and CBV, indicating a closer link between oxygen and glucose utilization and brain damage. Patients with minimal injury exhibited weak correlations, while patients with moderate to severe injuries displayed stronger correlations, emphasizing the critical role of oxygen and glucose metabolism in brain damage progression.

Table of Contents

Chapter 1: Introduction

I. Background

Cardiac arrest is a leading cause of death in the United State contributing to 5.6% of all deaths annually. **(Chugh et al., 2004)** Alarmingly, about 50% of short-term cardiac arrest survivors succumb in a permanent coma and 10-30% of long-term survivors endure irreversible brain damage. **(Safar, 1993)** Brain injuries after cardiac arrest are the cause of death in 68% of out-of-hospital patients and 23% in in-hospital patients. **(Laver et al., 2004)** These devastating outcomes are largely due to hypoxia resulting from transient global brain ischemia, a critical consequence of cardiac arrest. **(Xu et al., 2010)** While there have been many advancements in cardiac care, the long-term neurological impacts of post-cardiac arrest injuries still require more investigation. **(Nolan et al., 2008)**

Patients who have been resuscitated from cardiac arrest often remain unconscious for extended periods of time.**(Edgren et al., 1994)** The persistence of unconsciousness can indicate a range of conditions from a minor metabolic disruption to severe, permanent brain damage. Neurologists play a crucial role in predicting the neurological outcomes for these patients, a task with many challenges and minimal margin for error. Incorrect prognoses can have significant consequences: prediction of a poor outcome erroneously might lead to withholding potentially life-saving treatments, while optimistic outcomes can take up unnecessary time, money, and resources.

The responsibility to accurately predict the neurological outcomes of these patients encourages neurologists to employ a variety of tools such as neuroimaging and chemical biomarkers to maximize the specificity of their assessments. Emerging research has underscored

this multifaceted nature of post-resuscitation assessment where alterations in cerebral blood flow (CBF), intracerebral pressure dynamics, and oxygen delivery as contributors to cell death. **(Basu et al., 2003) (Nolan et al., 2008) (Chalkias et al., 2012)** This recognition of complexity has prompted a shift towards the development of more nuanced management strategies to predict neurological outcomes.

II. Thesis Overview

The inherent complexity of these post-resuscitation assessments underlines the importance of thorough research into each aspect of the process. Despite advancements in the field of cardiac arrest and resuscitation, post-cardiac arrest brain injury remains a common cause of morbidity and mortality. **(Nolan et al., 2008)** This thesis aims to investigate the effectiveness of various metabolic characteristics to distinguish between different brain states. This will be done by elucidating the correlation between brain injury patterns observed in comatose patients following a cardiac arrest event and metabolic measurements found in healthy individuals. Key metabolic parameters that will be examined include cerebral blood flow, cerebral blood volume, cerebral metabolic rate of oxygen, and cerebral metabolic rate of glucose.

Establishing the existence and strength of relationships between metabolic regulation and brain injury pathology can offer potential insights into the effects of metabolism change on brain injury during a cardiac arrest. This may prove to be a crucial component for clinical decision support systems, offering a basis for developing algorithms that could predict patient trajectories and guide treatment plans. This information could be pivotal in determining the urgency and nature of interventions, thereby optimizing resource allocation and potentially enhancing the speed and effectiveness of recovery protocols.

The range of metabolism characteristics that will be compared also allows precise conclusions that can better inform clinical-decision making. By examining multiple levels of healthy cerebral metabolism and its association with brain injury, we can attain a more comprehensive understanding of the underlying pathophysiology and its patterns. This approach not only enhances the ability to assess neurological function, but also contributes to precision medicine, offering the opportunity to tailor interventions and predictions to individual patient needs.

Three layers of increasingly complex analysis were done. In the first analysis, the correlations between lesioned areas of the brain were compared with each of the metabolism maps. This was repeated with the areas of the brain that were considered to not be lesioned. The second analysis took this a step further by using the k-means elbow clustering method to group brains with a similar percentage of injury to the whole brain. The median of correlations between lesioned areas of the brain with each of the metabolism maps was taken for each cluster. The same was repeated with the non-lesioned areas of the brain. Finally, an atlas that parcels the brain into Brodmann areas was applied to all patient brains and metabolism maps. The k-means elbow clustering method was repeated by grouping brains with similar percentage of injury through each of those Brodmann regions. The correlations of each region between brain maps for each were calculated.

III. Thesis Structure

This thesis is structured into several chapters, starting with Chapter 2: Related Works which gives a detailed review of the literature around the metabolic processes and brain injury. This is followed by Chapter 3: Methods that describe the brain datasets and atlas used as well as

an overview of the study design including any techniques and technologies used. Subsequently, Chapter 4: Results will present the data including numerous visualizations of the data on plots and tables. Finally, Chapter 5: Discussion will interpret the results of the data and propose rational for patterns in the data. It will discuss what these results could mean for potential future work.

Chapter 2: Related Work

This chapter reviews work related to post-cardiac arrest brain injury's relationship with metabolism in the brain. The specific metabolism characteristics of interest are cerebral blood flow, cerebral blood volume, cerebral metabolic rate of oxygen, and cerebral metabolic rate of glucose. In addition, the role of apparent diffusion coefficient in assessing brain injuries is discussed.

I. Overview of Metabolism in the Brain

Blood flow, oxygen, and glucose are common characteristics that are studied when looking at the metabolism of the brain. This a review of the numerous studies that look at different measurements of metabolism throughout the treatment process of cardiac arrest patients, patients in comatose state, and patients with any kind of traumatic brain injury.

a. CBF and CBV

Reperfusion is the restoration of blood flow to an area of the body that had been deprived of blood supply. After a cardiac arrest, reperfusion is essential to restore blood flow and limit ischemic damage. There are three stages of cerebral blood flow (CBF) alterations after resuscitation from cardiac arrest. CBF is observed to be the lowest on the day of injury, indicating minimal flow. **(Kelly et al., 1997) (Iordanova et al., 2017) (van der Brule, et al., 2018)**

This phase is followed by a brief period of cerebral hyperemia, where blood flow temporarily exceeds normal levels. While this may seem beneficial, the excessive blood flow can

be harmful. During hyperemia, the blood-brain barrier can become more permeable, potentially leading to edema and increased intracranial pressure. **(Bouma and Muizelaar, 1992)** This pressure can further damage the already vulnerable brain tissue contributing to secondary brain injury.

The hyperemic phase then transitions into cerebral hypoperfusion, a state of reduced blood flow that can last an extended period. During this phase, the sustained low CBF can exacerbate brain injury by perpetuating the cycle of ischemia and neuronal death. Ultimately, CBF may stabilize, but it can also persist in hypoperfusion, shift to global hyperemia, or cease entirely, leading to brain death. **(Buunk et al., 2000)**

Rapid restoration of blood flow is crucial after a cardiac event, as it often leads to better neurological outcomes. **(Esdaille et al., 2020) (Olasveengen et al., 2020)** In addition, CBV has been shown to be reduced in proportion to CBF following a severe brain injury. **(Marmarou et al., 2000)** This suggests that the regions of the brain with less blood flow and volume correlate with more severe injury. **(Thijs et al., 2002)** In hyperacute stroke patients, it has even been suggested that lower CBF values could predict further lesion growth. **(Fiehler et al., 2002)**

b. $CMRO_2$

More than half of energy consumed by the brain is used for synaptic function. **(Bouma and Muizelaar, 1992)** During conditions like a coma, where synaptic function has been reduced, the cerebral metabolic rate of oxygen ($CMRO_2$) - the amount of oxygen gas extracted from the blood by the brain - gets reduced to half of its normal level. This reduction in $CMRO_2$ is critical, as neuronal death can occur when oxygen utilization gets too low.

In the event of a cardiac arrest, CBF is decreased, but $CMRO_2$ is initially stable because the brain will compensate by extracting more oxygen from the blood. However, as long as CBF continues to decrease, a pattern also observed in about half of patients with acute head injuries, $CMRO_2$ begins to decrease as well. **(Cold, 1986)** This hypoxia is associated with less favorable outcomes, emphasizing the importance of oxygen for the brain's survival. **(Bardt et al., 1998)** This significance is further supported by the reduced mortality in traumatic brain injury patients after aggressive cerebral oxygenation. **(Narotam et al., 2009)** These findings suggest that management of oxygen levels and ensuring adequate cerebral oxygenation may be crucial in mitigating brain damage. While low oxygen levels seem to be a great indicator of brain damage and poor neurological outcome, the implications of high $CMRO_2$ levels are not as straightforward. High $CMRO_2$ levels could reflect increased metabolic activity in the brain, potentially as a compensatory response to stress or injury. This increased activity does not necessarily translate to beneficial outcomes or reduced brain injury.

c. CMR_{glu}

Glucose is essential for maintaining homeostasis in the adult brain. In cases of hypoglycemia, subjects typically experience a progression into lethargy, stupor, and eventually coma, as plasma glucose levels decreased or when the duration of hypoglycemia increased. **(Albers, 1972) (Dienel, 2019)** Promptly elevating glucose levels in these patients rapidly reversed these effects. This observation suggests that post-cardiac arrest comatose patients likely exhibit decreased cerebral glucose levels. Furthermore, studies indicate that in comatose survivors of out-of-hospital cardiac arrest who exhibit higher mean blood glucose levels during the first days of admission were associated with increased rates of death or severe neurological

impairment. **(Russo et al., 2018)** Elevated levels of glucose in the blood may signify inadequate glucose uptake by the brain, supporting the idea that severely injured brains demonstrate lower cerebral glucose levels.

A potential complication that can occur when adjusting glucose levels in a patient is the inadvertent recreation of the condition that is being treated. Individuals vary in their metabolic and nutritional status and administering excessive glucose into a hypoglycemic patient may result in hyperglycemia. **(Brooks and Martin, 2015)** An approach to this would be to monitor glucose production rate instead and allow autoregulatory mechanisms in the body to maintain glucose levels. **(Glenn et al., 2003)**

d. Relationship of Brain Injury and Metabolism

A more injured brain typically leads to poorer neurological outcomes, but the specific effects of cardiac arrest vary among different types of neurons and brain regions. This variability results in distinct injury patterns among cardiac arrest survivors. For instance, the hippocampal CA1 pyramidal neurons in the mesial temporal lobe are particularly susceptible to injury. **(Larsson et al., 2001) (Bjorklund et al., 2014)** This vulnerability often leads to memory impairments, especially for short-term memory, even among cardiac arrest patients who otherwise experience favorable outcomes from cardiac arrest. **(Tiainen et al., 2015) (Sabedra et al., 2015)** Neuronal types like these can influence deviations in expected metabolic levels and the severity of brain injury.

In the case of the same CA1 cells, ischemic damage to presynaptic components is associated with a decrease in glucose metabolism whereas damage to postsynaptic components is linked to an increase. **(Jorgensen et al., 1990)** This indicates a complex relationship between

neuronal damage and metabolic response and may blur the expected relationship between brain injury and metabolism.

II. Apparent Diffusion Coefficient

Diffusion-weighted images (DWI) leverages the sensitivity of MRI signals to the diffusion of water molecules within brain tissue. The intensity of this signal represents the amount of water molecules that diffuse through each voxel. **(Le Bihan et al., 1986) (Larsson et al., 1992)** This technique is notable for its rapid acquisition and processing time of these images providing clinicians a quick tool for analyzing images, which is critical in time-sensitive conditions.

A prominent clinical application of DWI is the rapid diagnosis of acute cerebral ischemia in acute brain stroke patients. **(Moseley et al., 1990)** The rapid diagnosis is possible because of the decreased apparent diffusion coefficient (ADC) values observed in affected brain regions, typically indicative of cell swelling, a common response to ischemia. **(Sotak, 2004)** The change in ADC values allows for prompt identification of ischemic tissues, facilitating immediate intervention.

Furthermore, there is growing evidence, particularly from animal studies, to show that there is a correlation between ADC values and underlying tissue structure. **(Chenevert et al., 2000)** This correlation has practical applications in identifying and characterizing lesions in the human brain. For instance, a study demonstrated that setting a maximum threshold for ADC values could successfully identify low-grade ductal carcinoma in the breast, achieving 100% specificity. **(Iima et al., 2011)** This highlights the potential of diffusion-weighted imaging in

diagnosing acute brain conditions and effectively detecting lesions based on tissue diffusion characteristics.

a. Injury Threshold

In diffusion-weighted MRI images, ADC values below 650 mm^2/s are often considered indicative of hypoxic-ischemic brain injury following cardiac arrest. Research has shown that ADC values are associated with more severe brain damage. Findings from multiple studies support the validity of using these thresholds for assessing the severity of brain injuries and their likely impact on patient recovery. **(Mlynash et al., 2010) (Wijman et al., 2009)**

The concept of using an ADC threshold to identify injured areas of the brain can be effectively applied to cardiac arrest patients. Research has shown that grouping comatose post-cardiac arrest survivors by the percentage of brain volume with an ADC value below 650-700 mm^2/s enhances the sensitivity of predicting poor outcome by 38%, while maintaining a specificity of 100%. **(Wijman et al., 2009)** This ADC threshold of below 650 mm^2/s continued to be consistently effective in differentiating patients with good and bad outcomes in single-center and multicenter cohorts. **(Hirsch et al., 2016) (Hirsch et al., 2020) (Yoon et al., 2023)**

This ADC-based approach offers a quantitative and objective method for assessing brain injury severity immediately following cardiac arrest. By setting an ADC threshold, areas of the brain that are associated with poor neurological outcomes could be quickly identified, thus enabling more targeted analysis at the voxel level.

Chapter 3: Methods

I. Datasets

In this work, one clinical dataset from the University of California, San Francisco and Zuckerberg San Francisco General Hospital Institutions, one research dataset from the neuromaps brain repository, and a parcellation scheme from the Conte69 atlas was used.

a. ADC MRIs of post-cardiac arrest comatose patients

The clinical dataset featured 83 patients who were treated at a single university-affiliated hospital. **(Calabrese et al., 2023)** These patients were retrieved by first identifying subjects between 2016 and 2021 who had fallen into a comatose state after suffering a cardiac arrest. These post-cardiac arrest patients were defined by having a Glasgow Coma Scale score of less than 8 after return of spontaneous circulation. Patients were then selected if they had brain MR imaging as part of the procedure. This is a routine multimodal prognostic evaluation for patients who are still unconscious.

The raw brain images were preprocessed and skull stripped resulting in a volumetric white matter brain in Montreal Neurological Institute 152 (MNI-152) space with a resolution of 1mm. For this study, the apparent diffusion coefficient (ADC) white matter diffusion-weighted imaging (DWI) brains were identified and used. Patients had varying degrees of injury as a result of hypoxia.

b. Metabolism-related brain annotations

The research dataset was derived from neuromaps, a python toolbox developed to assist researchers in conducting statistical comparisons between brains. **(Markello et al., 2022)** Neuromaps includes a large repository of brain datasets previously published by other researchers. These datasets, or annotations are available in the one of the four brain imaging spaces: MNI-152, FreeSurfer average brain (fsaverage), FreeSurfer to Conte69 left-right symmetric (fsLR), and Computerized Imaging and Visualization Environment Toolbox (CIVET). To facilitate the comparison of brain data across different datasets, Neuromaps provides python utilities that enable transformations between these imaging spaces. These include volume-to-surface transformations (registration fusion) and surface-to-surface transformations (multimodal surface matching). **(Buckner et al., 2011) (Wu et al., 2018) (Robinson et al., 2014) (Robinson et al., 2018)**

Four brain annotations associated with metabolic values were retrieved from Neuromaps. The brain annotations represented cerebral blood flow (CBF), cerebral blood volume (CBV), cerebral metabolic rate of oxygen ($CMRO_2$), cerebral metabolic rate of glucose (CMR_{glu}). **(Raichle et al., 2010)** The annotations were sourced from a study that measured regional distribution of aerobic glycolysis to better understand the role of glycolysis in the resting activity of the adult human brain and its relationship with established functional areas. 33 neurologically normal right-handed adults (19 women and 14 men) aged 20-33 years old in resting awake state were imaged with positron emission tomography. For each metabolic measure, each patient's scan was aligned with each other and then aligned to a target image that represents the Talairach space. **(Lancaster et al., 1995)** The resulting brain annotations were in fsLR surface space with a resolution of 164k vertices.

c. Brodmann areas parcellation scheme from the Conte-69 atlas

The "Conte-69" atlas was created with focus on the hemispheric asymmetries of the cerebral cortex for surface-based analysis. **(Van Essen et al., 2012)** The key features of this atlas include being high-resolution, surface-based mapping, and compatibility with many brain image formats. It supports a wide range of applications including detailed anatomical and functional analysis with multimodal integration. The Brodman parcellation scheme provided by the Conte69 atlas was used to define regions of interest for analysis. **(Brodmann, 1909)** These parcellations define cortical regions based on cytoarchitecture which is valuable for localization of cortical functions. Comparison of the relationship between these regions of interest (ROI) across brains allows for more precise and accurate calculations that a whole brain analysis may fail to represent. The Brodmann parcellation scheme identifies 43 total regions. 43 of these regions are labeled Brodmann areas and one region is reserved for the medial wall. Regions varied in size and were not uniform.

II. Design

Analysis of the brain annotations can be divided into 3 sections: whole brain lesion comparison, patient clustering by injury percentage, and voxel clustering by ADC value.

a. Initial Brain Transformations

The initial step of the study was transforming the brain maps into a unified image space for compatibility. The Brodman parcellation scheme from the Conte69 atlas is in the fsLR 32k space, so this would be the target image space for all brain annotations.

In transforming the clinical dataset of 83 ADC brains in MNI-152 1 mm space to fsLR 32k space, the neuromaps python function, neuromaps.transforms.mni152_to_fslr() was leveraged. This function linearly projects the image in MNI152 space onto an fsLR surface resulting in 83 ADC brains in the fsLR 32k surface space.

For the transformation of the research dataset with four metabolism-related brain images, another neuromaps python function, neuromaps.transforms.fslr_to_fslr() was used. The metabolism-related brain images were already in the fsLR image space, however it was in a different density. The metabolism-related brain images had a density of 164,000 vertices and the target space was a density of 32,000 vertices. This python function would linearly resample both hemispheres of the brain to a density of 32,000 vertices. The result is four metabolism-related brain images (cbf, cbv, cmr02, cmruglu) in the fsLR 32k surface space.

The transformation to fsLR 32k surface for a brain resulted in two GIFTI files. Each GIFTI file stores information about the ADC or metabolism-related value at each vertice of the brain for one hemisphere.

b. Whole Brain Lesion Comparison

The goal of whole brain lesion comparison is to directly compare the correlation of injured and uninjured areas of patient brains to normal metabolism brains. This would be a simple way to discover any global relationships between brains.

i. Masking the lesioned and non-lesioned parts of each patient brain

Using the 650 mm^2/s threshold, each ADC brain was dissected into two regions - lesioned and non lesioned and brain masks were generated. In addition, the medial walls of both brains

were sectioned out and removed from correlation calculations. This medial wall was determined by excluding any voxel from each brain with a metabolism value of 0.

The lesion brain masks were applied to each of the four metabolism maps. The result is a metabolism brain map that had the original metabolism value at voxels that were lesioned in the ADC brain, and a value of 0 at every other voxel. The same technique was repeated with the non-lesion brain masks to get metabolism brain maps that had the original metabolism value at voxels that were not lesioned in the ADC brain, and a value of 0 at every other voxel.

ii. Calculating Voxel by Voxel Correlations

To assess the normality of the distribution, the Shapiro-Wilk test was performed on the voxels of the ADC and metabolism brain. The test results indicated a non-normal distribution ($p < 0.05$), prompting the use of nonparametric methods for further analyses. Therefore, the Spearman's correlation coefficient was utilized instead of the Pearson's correlation to evaluate the relationships between sets of voxels, as it does not assume normality of the data.

For correlation calculations, voxels of value 0 were not included in the calculation, ensuring that only lesioned or non-lesioned voxels were considered in each calculation. Spearman's correlation coefficient is calculated for each pair of masked ADC and metabolism brains. This resulted in a total of eight correlation coefficients for each brain.

Across the 83 patient brains, the median of each of the eight correlation coefficients was taken. This resulted in eight final correlations that represent the median of lesion and non-lesion correlation coefficients between ADC values and cerebral blood flow, cerebral blood volume, cerebral metabolic rate of oxygen, and cerebral metabolic rate of glucose.

c. Patient Clustering by Injury Percentage

The dataset of brains is diverse and includes patients exhibiting a range of brain injury severities where some patients may be in a severely worse state than others. This variation may skew the representation of correlation coefficients across the entire dataset. To enable more focused and precise analysis, the k-means clustering algorithm was used to categorize brains into similar groups. By analyzing the median correlations within each cluster, deeper insights can be gained into the specific conditions prevalent within each dataset and derive correlation coefficients that are targeted towards each brain type.

i. K-Means elbow method clustering

To cluster patient brains with similar amounts of injury percentage, the k-means elbow method was used. The k-means elbow method is a heuristic for clustering that determines the optimal number of clusters within a dataset. It is performed by running the k-means algorithm across a range of *k* values and calculating the sum of squared errors (SSE). The error is the distance from a point and the centroid of the cluster assigned to that point. The calculations are plotted on a graph where the x-axis is the range of *k* values and y axis is the SSE. To identify the optimal *k* value or clusters, there will be a point in the plot where the SSE decreases much more slowly than the previous *k* values, also known as the "elbow." This k value is considered the optimal *k* value for that dataset.

After selecting the optimal number of clusters, the k-means algorithm is performed on the 83 patient brains. In this analysis, each patient is treated as a feature vector and will be clustered depending on the percentage of injured voxels of the whole brain. The k-means algorithm excels at partitioning a dataset into distinct non-overlapping clusters by iteratively adjusting the

centroids. It aims to minimize the variance within each cluster, resulting in the most representative centroid for each cluster. This method ensures that patients with similar injury profiles are grouped together, facilitating more targeted analyses based on the clustering results.

ii. Voxel Correlations by each Cluster

The voxel correlations in each brain had already been previously calculated. With additional information about similar brains, the median correlations of brains within each cluster can be calculated. For each metabolism brain, there should be *k* correlation coefficients that represent the median lesion correlation coefficients and *k* correlation coefficients that represent the non-lesion correlation coefficients of that cluster.

d. Patient Clustering with Brodmann Areas

Correlations across the whole brain may not take into account regional differences in ADC and metabolic values. This may give correlation coefficients that may not represent the whole picture of the brain. Sectioning patients with similar injury together and also brains into the Brodmann regions may give a better idea of how correlation coefficients may vary across both patients and brains.

i. Applying the Brodmann Area parcellations

The Brodmann Area parcellation assigns each vertex of an fsLR 32k brain to one of the Brodmann Areas or the medial wall encompassing a total of 43 regions. The coordinates of each vertex in the parcellation were extracted and then applied to the datasets of 83 patient brains and

four metabolism-related brains. Consequently, each of these 87 brains was mapped with 32,000 vertices categorized into the 43 distinct regions.

ii. Calculating percentage of injury across Brodmann Areas

As used previously for whole brain lesion comparisons, the same 650 mm^2/s ADC value threshold was used to determine injured voxels. In a patient ADC brain, each region was given an injury percentage that was calculated by dividing the number of total voxels in that region by the number of voxels below 650 mm^2/s. The result is 83 patient brains with 43 injury percentages for each of the 43 Brodmann Area parcellations.

iii. K-Means elbow method clustering

The same clustering method for the previous patient brains, k-means elbow method clustering, is applied. In this method, the optimal *k* value, which represents the number of clusters, is chosen and used to group patient brains with similar injury percentages. In this iteration, however, the brain is divided into 43 regions, which can give more information to use for clustering. Instead of a single percentage of injury that represents the whole brain, 43 percentages of injury that represent the 43 regions of the brain will be used to group the brains.

iv. Calculating Regional Correlations

For all brain maps within each cluster, the correlations for each brain region was calculated between the ADC brain maps and metabolism brain maps from each of the four healthy subjects. This statistical approach ensures that for every region, the central tendency of the correlation values is determined, effectively reducing the impact of outliers.

Spearman's correlation coefficient was taken between ADC values and metabolism values for each of the 43 regions. Accompanying each correlation coefficient, a p-value was derived from a t-distribution with n-2 degrees of freedom where *n* is the number of voxels in that region. This analysis resulted in 83 brains categorized into one of *k* clusters. For each brain, a total of 172 correlation coefficients and p-values were computed, corresponding to the 43 regions across 4 metabolic measures. To reduce the complexity of the analysis, the four most injured regions of each cluster will be selected and compared across regions.

Chapter 4: Results

This chapter is divided into three major sections: one for each set of analyses. The first analysis compares the lesioned and non-lesioned areas of the whole brain. The second analysis differentiates brains by the percentage of brain volume that is injured before comparing lesioned and non-lesioned areas of the whole brain. The third analysis also differentiates brains by the percentage of brain volume that is injured, but across 43 parcels of the brain before calculating correlation coefficients. Data is presented in tables and graphs, and also plotted on a 3D visual of the brain to better visualize comparisons.

I. Whole Brain Lesion Comparisons

These correlations between lesion and non-lesion focuses provide a broad overview of the correlations between lesioned and non-lesioned brain regions relative to normal metabolic brain activity. Spearman's correlation coefficient is used to analyze voxel-by-voxel data across 83 patient brains. The results of the analysis are presented in **Table 1**. where each correlation coefficient represents a median value derived from pairs of masked ADC and metabolism brain maps. These findings can identify potential global relationships and abnormalities in brain metabolism associated with lesioned areas.

median correlation coefficients (*r*)	**CBF**	**CBV**	**$CMRO_2$**	**CMR_{glu}**
Lesioned	-0.018	0.015	-0.080	-0.057
Non-Lesioned	0.030	0.014	-0.054	-0.057

T**able 1: Medians of Spearman's correlation coefficients:** The table summarizes the Spearman correlation coefficients for lesion and non-lesioned brain regions across 83 patient brains rounded to the nearest thousandth. The table table displays the median correlation values between ADC and four metabolic parameters: cerebral blood flow (CBF), cerebral blood volume (CBV), cerebral metabolic rate of oxygen ($CMRO_2$), and cerebral metabolic rate of glucose (CMR_{glu}) for both lesioned and non-lesioned areas.

a. Cerebral Blood Flow (CBF)

The negative correlation in lesioned areas suggests a slight inverse relationship between ADC values and CBF, implying that higher diffusion may correspond to lower blood flow in lesioned regions. Conversely, the positive correlation in non-lesioned areas, although weak, indicates a direct relationship, where regions with higher diffusion coefficients might experience slightly increased blood flow.

b. Cerebral blood volume (CBV)

Both lesioned and non-lesioned areas show very weak positive correlations with CBV. This suggests minimal impact of ADC values on the blood volume, with slightly higher diffusion potentially corresponding to slightly higher blood volume in both types of tissue.

c. Cerebral metabolic rate of oxygen ($CMRO_2$)

Both areas exhibit negative correlations, which is more pronounced in the lesioned areas. This indicates a stronger inverse relationship in lesioned regions, where increased diffusion is

associated with significantly reduced oxygen metabolism. This might reflect more severe metabolic disruption in lesioned brain tissue.

d. Cerebral metabolic rate of glucose (CMR_{glu})

The equal negative correlation coefficients suggest a uniform inverse relationship across both lesioned and non-lesioned areas between ADC values and glucose metabolism. This indicates a consistent pattern where regions with higher diffusion exhibit reduced glucose metabolism across all regions of the brain, lesioned or non-lesioned.

The median correlation coefficients across different metabolism measurements reveals a complex relationship between metabolism and brain injury. The negative correlations in lesioned regions across oxygen and glucose metabolism rates are notable and suggest that lesion might lead to significant metabolic disruptions. The correlations in non-lesioned areas are generally weaker, indicating less variability and impact on metabolism, which is consistent with expected normal functioning of these regions.

II. Patient Clustering by Injury Percentage

The previous results gave a broad overview of relationships between large regions of each brain. To better elucidate the complex dynamics of brain injuries and their metabolic impacts, a refined analysis that accounts for variability in injury severities among patients was conducted. The diverse severity of brain injuries across patients could skew the overall representation of correlation coefficients, so the k-means clustering algorithm was employed. This approach allows the segmentation of the dataset into clusters of patients with similar brain injury profiles. By focusing on these homogenous groups, more precise correlation coefficients

can be derived which gives deeper insights of the relationship between brain injury and metabolism among specific conditions.

a. K-Means Elbow Method

To categorize patient brains into clusters based on similar injury severities, the k-means elbow method clustering method was utilized. This method helps determine the optimal number of clusters by calculating and plotting the sum of squared errors (SSE) for a range of cluster numbers (k). The "elbow" point of this plot, where the rate of decrease in SSE significantly drops, indicates the most appropriate number of clusters for our dataset. **Figure 1** shows these SSE graphed over k value range of 1 through 10. The plot shows a steep decline across 1 to 3 clusters. After 3 clusters, the difference of SEE significantly decreases, appearing to be almost flat. Therefore, at k=3 is the elbow point and is also the optimal number of clusters for segmenting the dataset of brains by percent injury.

Successful clustering of patient brains resulted in the formation of three distinct clusters, each representing varying severity of injuries. The first cluster, comprising 50 brains, exhibited a median injury level of about 1.0% of voxels. The second cluster, comprising 16 brains, exhibited a median injury percentage of 32.2% of voxels. The final cluster, comprising 17 brains, exhibited 68.2% of voxels.

In summary, the three clusters can be categorized as minimal injury, moderate injury, and severe injury, respectively with a majority of brains representing minimal injury. Across each cluster, the median correlation coefficients of each metabolism and ADC brain pair for lesioned and non-lesioned parts of the brains were taken again. **Table 2.** illustrates the resulting median correlation coefficients.

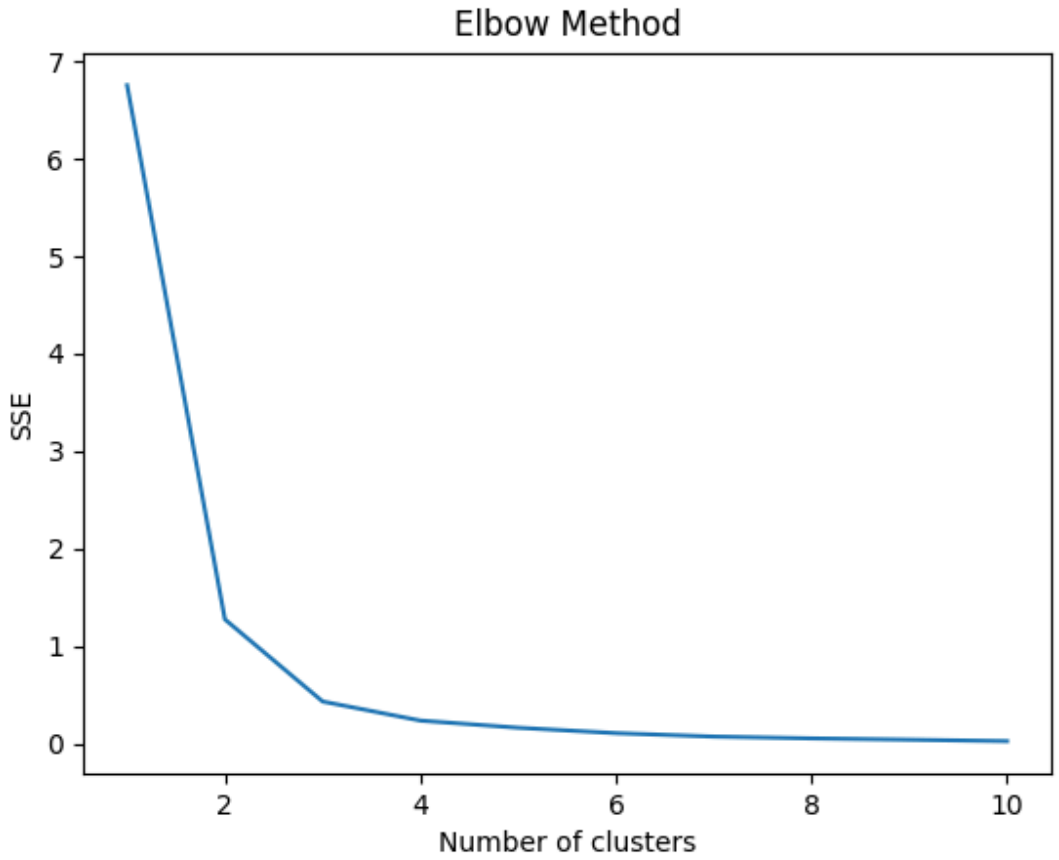

Figure 1. Elbow Method Plot for Optimal Cluster Determination: The plot illustrates the sum of squared errors (SSE) as a function of the number of clusters used in the k-means clustering algorithm. The "elbow" point, where the rate of decrease in SSE significantly flattens, appears around 3 clusters, suggesting that this is the optimal number of clusters for segmenting the dataset of patient brains based on injury severity. This point marks where additional clusters do not significantly improve the clustering effectiveness, thereby guiding the selection of k=3 for subsequent analyses.

Median Correlation Coefficients (*r*) for each Cluster	**Cluster 1 (minimal injury)**	**Cluster 2 (moderate injury)**	**Cluster 3 (severe injury)**
Lesioned CBF	-0.031	-0.015	0.004
Non-lesioned CBF	0.055	-0.004	-0.094
Lesioned CBV	0.004	0.050	0.018
Non-lesioned CBV	0.004	0.011	0.076
Lesioned $CMRO_2$	0.008	-0.127	-0.185
Non-lesioned $CMRO_2$	-0.036	-0.097	-0.155
Lesioned CMR_{glu}	-0.014	-0.106	-0.095
Non-lesioned CMR_{glu}	-0.044	-0.078	-0.198

Table 2. Summary of Median Correlations of each Metabolism Brain by Cluster: This table presents the median correlation coefficients for cerebral blood flow (CBF), cerebral volume (CBV), cerebral metabolic rate of oxygen ($CMRO_2$), and cerebral metabolic rate of glucose (CMR_{glu}) across three clusters categorized by injury severity: minimal, moderate, and severe. The values reflect the median correlations for both lesioned and non-lesioned brain areas with each cluster, highlighting how metabolic responses vary with the extent of brain injury. The values are rounded to the nearest thousandth.

b. Cerebral Blood Flow (CBF)

In cluster 1, lesioned CBF shows a slight negative correlation (-0.031), suggesting an elevated blood flow in lesioned areas, while non-lesioned areas show a positive correlation (0.055), indicating that areas of elevated blood flow are more likely to result in no injury. Both areas show a correlation with high CBF values. The strong positive correlation in non-lesioned areas may be because the whole brain has very little injury and the general trend of healthy metabolic values is positive. The negative correlation in lesioned values may be more significant in showing the relationship between low ADC and high CBF values, but overall, there is not a clear pattern.

In cluster 2, both lesioned (-0.015) and non-lesioned (-0.004) CBF correlations are slightly negative, but close to zero. Lesioned areas have a slightly stronger correlation than non-lesioned areas, but the difference is very small.

In cluster 3, lesioned CBF correlations are very close to zero (0.004), while non-lesioned correlations are stronger and negative (-0.094). The strong negative correlation means that high ADC values were associated with low CBF values. This should reinforce the idea that areas of higher metabolism should be more injured, however lesioned correlations were weak. The weak correlations may be due to most regions of the brain being injured without a clear pattern.

c. Cerebral Blood Volume (CBV)

In cluster 1, both correlations are very weak (0.004, 0.004), suggesting that there is no clear pattern between injury and CBV. Unlike cluster 1 in CBF, there is not a strong positive correlation in the non-lesioned areas despite minimal injury across the brains.

In cluster 2, lesioned correlations were strongly positive (0.050), meaning that low ADC values were associated with low cerebral blood volumes in a healthy brain. Similarly, non-lesioned correlations were also positive, but not as strong (0.011), meaning that high ADC values were associated with high CBV values. This trend in CBV was inversely true for CBF in cluster 2 (-0.015, -0.004). An explanation for this pattern is a relationship where areas of high blood volume tend to have lower blood flow.

In cluster 3, the same trend as before is seen where the CBV correlations are the inverse of CBF correlations. Lesioned CBV (0.018) and non-lesioned CBV (0.075) show positive correlations whereas lesioned CBF (0.004) and non-lesioned CBF (-0.094) had weak or strong negative correlations. The positive correlations in both areas reinforces the conclusion from

cluster 2 that low ADC values are associated with low CBV values and high ADC values are associated with high CBV values.

d. Cerebral Metabolic Rate of Oxygen ($CMRO_2$)

In cluster 1, the correlation for lesioned areas (0.008) was slightly positive but very weak. The weak correlation may be due to the low amount of injured regions in this cluster. The correlation of non-lesioned areas (-0.036), which accounted for more than 90% of the brains, was a little stronger, but it did seem significant. Both correlations were very weak overall.

In cluster 2, both lesioned (-0.127) and non-lesioned (-0.097) areas show weakly moderate negative correlations. These correlations support the idea that brain injury (low ADC values) may be associated with higher metabolic activity.

In cluster 3, both lesioned (-0.185) and non-lesioned (-0.155) correlations are negative and even stronger than cluster 2. This is surprising where even in brains that are severely injured across most of its regions, the correlations will stay strong. The strong negative correlations reinforce the conclusion of cluster 2 that brain injuries are associated with higher $CMRO_2$ values.

e. Cerebral Metabolic Rate of Glucose (CMR_{glu})

In cluster 1, both correlations are negative where the non-lesioned correlation (-0.044) was stronger than the lesioned correlation (-0.014). The difference in strength of the correlation may be due to the median percent of brain injury in this cluster was around 1%.

In cluster 2, both correlations were both strong and negative where lesioned correlation (-0.106) was stronger than non-lesioned correlation (-0.078). The same trend seen in $CMRO_2$

clusters is seen in CMR_{glu} clusters where both lesioned and non-lesioned correlations are very strong and negative.

In cluster 3, this conclusion is still reinforced. Both correlations are strong and negative, but with an interesting twist where the non-lesioned correlation (-0.198) is stronger than the lesioned-correlation (-0.095). The non-lesioned correlation coefficient here is the strongest correlation coefficient seen so far. It seems that $CMRO_2$ and CMR_{glu} correlations may be better associated with brain injury especially in patients with moderate to severe injuries. The strong correlations also tend to be negative which reinforces the idea that high metabolic values are associated with low ADC values, or brain injury.

III. Patient Clustering with Brodmann Areas

To further explore the regional differences in ADC and metabolic values, a methodical approach involving Brodmann Area parcellations and patient clustering was employed. This approach extended on the patient clustering by percentage of injury by further dividing the percentage of injury into 43 regions in the brain. The goal of this approach was to see if there were regional differences in correlation that may affect the previous analysis.

First, the Brodmann Area parcellation was applied to map 87 brains (83 patient brains and 4 metabolism-related brains) into 43 distinct regions. Each region's injury percentage was calculated using a threshold ADC value of 650 mm^2/s. These injury percentages were then used in a k-means elbow method clustering to group patients with similar injury profiles. Finally, the regional correlations between ADC values and metabolic values was calculated using Spearman's correlation coefficients.

i. K-means Elbow Method

The k-means elbow method was deployed again to determine the optimal number of clusters for group patient brains based on the injury percentages 43 Brodmann Areas. **Figure 2.** visualizes the sum of squared errors (SSE) across a range of k values. From the graph, it appears that the "elbow" point is at k=4 where the difference of SSE becomes much less after this point than before. Therefore, the 83 patient brains were grouped into 4 clusters for the k-means clustering calculations.

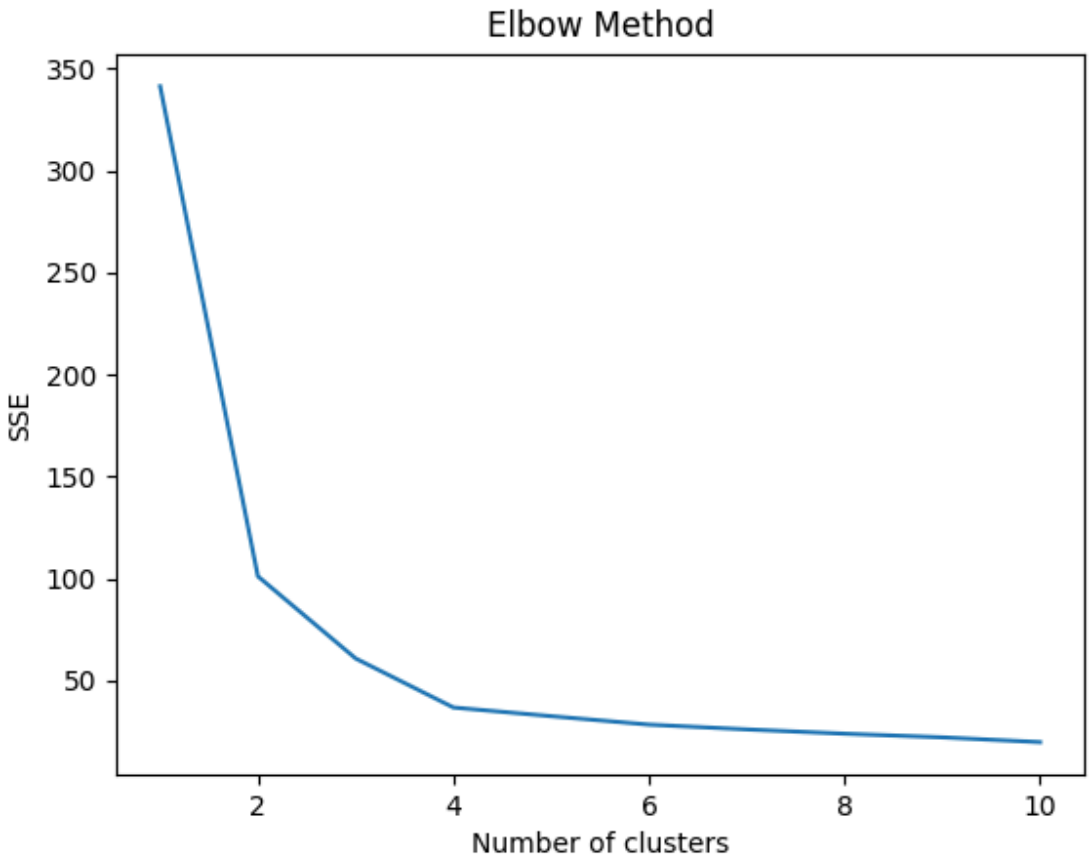

Figure 2. Elbow Method Plot for Optimal Cluster Determination: The plot displays the sum of squared distances (SSE) for the k values of 1 through 10. At k=4, the SSE begins to decrease more slowly, suggesting that it would provide a balanced and efficient representation of the data for subsequent analyses.

	Cluster #0 (minimal)	**Cluster #1 (moderate)**	**Cluster #2 (severe)**	**Cluster #3 (critical)**
Median Injury Percentage	0.1%	15.0%	68.5%	96.4%
Number of Patient Brains	49	15	14	5

Table 3. Summary of Brain Injury Severity Across Different Clusters: The table shows the results of clustering based on the median injury percentage for each region. Each cluster is described by its level of severity (minimal, moderate, severe, and critical), the median percentage of injury for brains in that cluster, and the number of patient brains included in each cluster.

The results of the k-means clusters are presented in **Table 3** where 49 of the 83 patient brains were grouped into Cluster #0 with minimal injury (0.1%). This was the largest amount of brains in a cluster. Cluster #1 consisted of 15 patients with a moderate amount of injury (15.0%). Cluster #2 consisted of 14 patients classified as having severe injury (68.5%). Cluster #3 had the least number of brains at 5 brains, with the most critical injury (96.4%). This distribution of patient brains showed a higher concentration of minimal injury brains with a substantial reduction in number of brains as severity increases.

The median of injury percentages for each brain region for each cluster was calculated and the results can be seen in **Appendix 1**. In each cluster, the four regions with the higher percentage of injury were taken. For Cluster 0, the regions that were found to have the highest injury percentage were Brodmann Areas 6 (1.3%), 3 (3.9%), 1 (4.1%), and 4 (7.6%). Brodmann areas 6 and 4 are associated with motor functions in execution of voluntary and involuntary movements. Brodmann Areas 3 and 1 are part of the primary somatosensory cortex and involved in processing of tactile information such as touch. All four of these Brodmann Areas are clustered on the dorsal parts of the frontal and parietal lobes.

In Cluster 1, the most injured regions were Brodmann Areas 4 (55.4%), 39, (56.3%) 19 (65.5%), and 18 (66.2%). Brodmann Area 4 was also seen in Cluster 0, and its main responsibility is the execution of voluntary motor movements. Brodmann Areas 18 and 19 play crucial roles in the visual processing pathway. Area 18 receives initial visual information from the primary visual cortex for preliminary processing, which is then sent to Area 19 for higher-order interpretation. Brodmann Area 39, located in the angular gyrus of the parietal lobe, is involved in spatial recognition and language processing. Collectively, Brodmann Areas 18, 19, and 39 are situated in the posterior regions of the brain, which are predominantly responsible for attention and visual functions.

In Cluster 2, the selected regions were Brodmann Areas 19 (93.5%), 2 (93.6%), 18 (94.7%), and 39 (95.4%). Brodmann Areas 18, 19 and 39 were also seen in Cluster 1, where they affected visual processing and attention. Brodmann Area 2 is part of the primary somatosensory cortex and interprets signals related to touch and pressure. This suggests that regions of the brain related to visual function could be the most vulnerable injury.

In Cluster 3, the four most injured Brodmann Areas were 8 (99.1%), 1 (99.1%), 3 (99.4%), and 5 (99.8%). Brodmann Area 8 is located in the frontal lobe and is involved in the execution of eye movements (saccades). Brodmann Areas 1, 3, and 5, located in the parietal lobe, are involved in processing somatosensory input signals. Brodmann Areas 1 and 3 processes initial input from sensory receptors before Brodmann Area 5 further processes that information to contribute to spatial awareness and motor planning. Although these areas may seem separate, eye movement and attention indirectly supports sensory functions. Brodmann Area 8 can

facilitate effective perception and processing of visual and spatial information which is important for the integration of sensor and motor signals.

After selecting specific regions of the brain within each cluster, Spearman's correlation coefficient was calculated between ADC values in that region and each metabolic value. This process was repeated for each cluster to identify the relationships between brain injury and metabolic parameters across different levels of injury severity. Although the four most injured regions were selected across the four clusters, ten distinct regions of the brain were identified overall, indicating overlap among clusters.

a. Cerebral Blood Flow (CBF)

Table 4. presents the median Spearman correlation coefficients between ADC values in damaged patient brains and CBV values in healthy brains across different Brodmann Areas and injury severity clusters. The correlation coefficients in white are the most injured regions in each cluster and are the regions of interest. In Cluster 0, BA1 shows a relatively strong positive correlation (0.191), indicating an association between minimal injury and higher CBF. BA3 (0.069), BA4 (0.015), and BA6, exhibit very weak correlations suggesting that minimal injury has very little association. BA18 also shows a strong positive correlation (0.193). This may indicate that BA18 and BA1 are regions that tend to be more vulnerable to injury.

In Cluster 1, BA4 shows a moderate negative correlation (-0.116), a contrast to Cluster 0, which may indicate that injury in this region may be caused by reduced blood flow during cardiac arrest. Similar changes to negative correlation occur in BA2 (-0.188), BA6 (-0.026), and BA8 (-0.062). BA18 maintains a strong and positive correlation (0.316) while other regions also responsible for visual function show a weaker positive correlation in BA19 (0.033) and BA39

(0.087). This may indicate that the posterior parts of the brain responsible for visual function may be more prone to injury.

Cluster 2 follows the same pattern as Cluster 1 where BA2 has a strong positive correlation (-0.153) which contrasts patients with minimal injury. BA18 shows a strong positive correlation with brain injury (0.320), but this time BA19 (-0.002) and BA39 (-0.029) show weak negative correlations, indicating almost no relationship. This reinforces the idea that BA18 is the most vulnerable region of the visual system. Another trend across clusters is BA5 has a gradual increase in correlation strength (0.248) as injury severity increases. This pattern continues into Cluster 3.

Similar to Cluster 0, patients with critical amounts of injury tend to have very weak correlations with a few dramatic exceptions. BA5, as mentioned before, shows a strong positive correlation (0.370) that seems to increase in strength as brain injury severity increases. BA6 and BA8, regions responsible for motor function, show a dramatic jump to a strong positive correlation (0.211) after having weak negative correlations in Cluster 1 and 2. BA18 continues to retain its strong positive correlation (0.154). In patients with critical injuries, these regions seem to exhibit associations with higher CBF values.

Median Correlation in CBF	Cluster 0 (minimal)	Cluster 1 (moderate)	Cluster 2 (severe)	Cluster 3 (critical)
BA1	0.191	0.054	-0.08	-0.024
BA2	-0.006	-0.188	-0.153	0.036
BA3	0.069	-0.087	-0.124	0.042
BA4	0.015	-0.116	-0.038	0.073
BA5	0.035	0.092	0.248	0.370
BA6	0.029	-0.026	-0.086	0.104
BA8	0.086	-0.062	-0.102	0.211
BA18	0.193	0.316	0.320	0.154
BA19	0.028	0.033	-0.002	-0.137
BA39	0.007	0.087	-0.029	-0.050

Table 4. Median Correlation with Cerebral Blood Flow (CBF) Across Brodmann Areas (BAs) in Different Injury Clusters: This table presents the median spearman correlation coefficients between ADC and CBF values for the four Brodmann Areas with the highest percentage of injury across four injury severity clusters: minimal, moderate, severe, and critical. The white regions represent the top four most injured regions in that cluster. The gray regions are the most injured regions of other clusters, but filled in for better comparison.

b. Cerebral Blood Volume (CBV)

In Cluster 0, most of the correlation coefficients in the somatosensory regions including BA1 (0.036), BA2 (0.048) and BA5 (0.037) have weak positive correlations. BA3 is also responsible for somatosensory function, but exhibits a moderate negative correlation (-0.132) indicating that this region, which is only 3.9% injured, is associated with low blood volume. BA8 also shows a strong positive correlation, which continues into the other cluster of brains, suggesting that this region is associated with higher cerebral blood volume.

In Cluster 1, the Brodmann Areas responsible for motor function: BA4 (0.104), BA6 (0.0.066), and BA8 (0.188) have moderate positive correlations. This may indicate motor functions are associated with lower blood volume in moderately injured patients. BA18 continues to have a strong positive correlation (0.179), indicating that it is also associated with lower blood volume and is more prone to injury. BA19 also continues to have a weak correlation (0.021), but this time, BA39 exhibits a strong negative correlation (-0.213). This may suggest that the decrease in blood volume causes brain injuries in this region. This region is also the only region that represents regions of the brain that control attention.

Cluster 2 exhibits many similar characteristics to Cluster 1. BA4 (0.120), BA6 (0.218), and BA8 (0.297) exhibit moderately strong positive correlations, which may indicate the regions associated with motor function exhibit increased sensitivity to injury. The somatosensory regions showed a mix of weak and strong correlations. BA1 (-0.033) and BA2 (0.056) had weak correlations while BA3 (0.135) and BA5 (0.169) had moderate positive correlations. BA3 processes initial sensory input and BA5 is involved in higher order processing and integration. BA1 and BA2 are intermediate steps in processing the signals. A possible theory is that the injuries caused to BA3 may affect the function of BA5. BA18 shows a strong positive correlation (0.227) and BA39 also now shows a strong negative correlation (-0.206) which may mean the injuries to regions of the brain associated with attention may be negatively affected by lack of blood volume.

In Cluster 3, weak correlations, positive or negative, are seen through each of the regions including BA1 (0.039), BA3 (-0.038), and BA5 (0.085). The correlation coefficient that is significantly different is BA8 which demonstrates a strong positive correlation (0.170). BA8, a region whose primary function is the control of voluntary eye movements, had a strong positive

correlation throughout each of the clusters and may be related to the vulnerability of the posterior region of the brain that is associated with visual function.

Median Correlation in CBV	Cluster 0 (minimal)	Cluster 1 (moderate)	Cluster 2 (severe)	Cluster 3 (critical)
BA1	0.036	-0.027	-0.033	0.039
BA2	0.048	0.061	0.056	0.082
BA3	-0.132	-0.006	0.135	-0.038
BA4	0.020	0.104	0.120	0.019
BA5	0.037	0.139	0.169	0.085
BA6	0.082	0.066	0.218	-0.056
BA8	0.150	0.188	0.297	0.170
BA18	0.021	0.179	0.227	-0.005
BA19	-0.088	0.021	0.020	-0.024
BA39	-0.049	-0.213	-0.206	-0.034

Table 5. Median Correlation with Cerebral Blood Volume (CBV) Across Brodmann Areas (BAs) in Different Injury Clusters: This table presents the median spearman correlation coefficients between ADC and CBV values for the four Brodmann Areas with the highest percentage of injury across four injury severity clusters: minimal, moderate, severe, and critical. The white regions represent the top four most injured regions in that cluster. The gray regions are the most injured regions of other clusters, but filled in for better comparison.

c. Cerebral Metabolic Rate of Oxygen ($CMRO_2$)

Cluster 0 had moderately weak correlations throughout each of its regions, with the exception of two strong positive correlations in BA1 (0.199) and BA18 (0.210). A strong positive correlation was also seen in cerebral blood flow, which may indicate a relationship where injury is associated with low blood flow and oxygen in this region. BA18 has consistently

shown positive correlations across metabolism values, and its strong correlation could be attributed to its susceptibility to injury.

Unlike previous correlation coefficients, most correlations in Cluster 1 are negative across regions. This may mean that brain injury is more associated with high $CMRO_2$ values in a healthy brain. The lack of oxygen in the brain may cause injuries across the brain. The exception is the strong positive correlation of BA18 (0.332) which reinforces this region as being more vulnerable.

Cluster 2 also has moderate to strong negative correlations across each region including BA2 (-0.145), BA19 (-0.103), and BA39 (-0.163). This suggests that brain injury in this region is caused by the lack of $CMRO_2$. BA18 maintains a strong positive correlation (0.312).

Median Correlation in $CMRO_2$	**Cluster 0 (minimal)**	**Cluster 1 (moderate)**	**Cluster 2 (severe)**	**Cluster 3 (critical)**
BA1	0.199	0.079	-0.108	-0.060
BA2	0.011	-0.215	-0.145	0.061
BA3	0.092	-0.096	-0.200	-0.046
BA4	0.027	-0.102	-0.082	0.134
BA5	0.023	0.125	0.227	0.389
BA6	-0.017	-0.117	-0.201	0.093
BA8	0.046	-0.102	-0.230	0.161
BA18	0.210	0.332	0.312	0.155
BA19	-0.027	-0.081	-0.103	-0.154
BA39	-0.042	-0.134	-0.163	-0.066

Table 6. Median Correlation with Cerebral Metabolic Rate of Oxygen ($CMRO_2$) Across Brodmann Areas (BAs) in Different Injury Clusters: This table presents the median spearman

correlation coefficients between ADC and $CMRO_2$ values for the four Brodmann Areas with the highest percentage of injury across four injury severity clusters: minimal, moderate, severe, and critical. The white regions represent the top four most injured regions in that cluster. The gray regions are the most injured regions of other clusters, but filled in for better comparison.

Cluster 3 has a dramatic variety of correlations. BA4 (0.134), BA5 (0.389), BA8 (0.161) and BA18 (0.155) have moderate positive correlations. In these patients, where more than 95% of the brain is injured, it suggests that brain injury is associated with low $CMRO_2$ values in healthy brains. However, this could also be a consequence of critical brain injury throughout the brain, making it difficult to draw definite conclusions about the cause of injury.

d. Cerebral Metabolic Rate of Glucose (CMR_{glu})

Table 7 outlines the correlation coefficients between CMR_{glu} and ADC values for the clusters. The pattern in CMR_{glu} correlation coefficients seem to echo patterns seen in $CMRO_2$. In Cluster 1, correlation coefficients are weak except for strong positive correlations in BA1 (0.199) and BA18 (0.210). BA1 in Cluster 0 also showed moderate positive correlations in other metabolic values, however it had weak correlations in other clusters. Since this cluster has low injury, this could be explained by the non-lesioned and higher ADC values tend to have stronger correlations with high metabolic values, but the lesioned and low ADC values do not have significant correlation strengths. The strong positive correlation observed in BA18 is consistent across various metabolic measurements and all injury clusters, suggesting a reliable association.

In Cluster 1, BA4 has a strong negative correlation (-0.227) suggesting that this region, responsible for execution of voluntary movements, may be damaged due to its dependence on glucose. This region also had a negative correlation with $CMRO_2$. The surrounding areas: BA2 (0.046), BA3 (0.087), and BA5 (0.081) had weak positive correlations, which is different from the expected negative correlations. This difference may further emphasize BA4's unique

association with CMR_{glu} and its heightened risk of injury compared to adjacent regions. BA18 has a strong positive correlation (0.204) and BA19 has a strong negative correlation (-0.208) which were patterns that were also observed in $CMRO_2$. The correlation of BA39 is strong and positive (0.359) which is a big difference from any values seen before.

Median Correlation in CMR_{glu}	**Cluster 0 (minimal)**	**Cluster 1 (moderate)**	**Cluster 2 (severe)**	**Cluster 3 (critical)**
BA1	0.200	-0.059	-0.053	0.034
BA2	-0.013	0.046	-0.194	0.017
BA3	0.067	0.087	-0.158	0.005
BA4	-0.079	-0.227	-0.176	0.017
BA5	0.008	0.081	0.272	0.345
BA6	-0.034	-0.083	-0.211	0.101
BA8	-0.009	-0.182	-0.319	0.113
BA18	0.170	0.204	0.196	0.111
BA19	-0.059	-0.208	-0.271	-0.207
BA39	0.046	0.359	0.160	0.013

Table 7. Median Correlation with Cerebral Metabolic Rate of Glucose (CMR_{glu}) Across Brodmann Areas (BAs) in Different Injury Clusters: This table presents the median spearman correlation coefficients between ADC and CMR_{glu} values for the four Brodmann Areas with the highest percentage of injury across four injury severity clusters: minimal, moderate, severe, and critical. The white regions represent the top four most injured regions in that cluster. The gray regions are the most injured regions of other clusters, but filled in for better comparison.

Cluster 2 also displays this pattern of BA18 having a strong positive correlation (0.195), BA19 having a strong negative correlation (-0.271), and BA39 having an oddly positive correlation (0.160). This suggests that injury in BA39, a region involved in language

comprehension, is not associated with the absence of glucose during cardiac arrest. There may be a higher metabolic reserve in BA39 within healthy patients.

In Cluster 3, the regions responsible for interpreting somatosensory signals had weak correlations including BA1 (0.034), BA2 (0.017), and BA3 (0.005). However, BA5 had a strong positive correlation (0.345) which is a trend that was also seen in $CMRO_2$. In this region, as injury severity increases, the strength of correlation increases. This suggests a strong association between injured voxels and metabolic values, which could be a marker for predicting the extent and impact of injuries in this region. BA19 showed a strong negative correlation (-0.207) which is a trend that has been consistent with Cluster 1 and Cluster 2.

Chapter 5: Discussion

Post-resuscitation assessments are complex and have small margins of error for prognosis. The study aimed to focus on metabolic values: cerebral blood flow, cerebral blood volume, cerebral metabolic rate of oxygen, and cerebral metabolic rate of glucose and their relationship with brain injury following cardiac arrest. By employing a multi-level approach, distinct patterns of metabolic disruption associated with different extents and regions of brain injury were uncovered.

I. CBF and CBV are Weakly Correlated With Brain Injury

CBF and CBV showed weaker correlations with low ADC values than $CMRO_2$ and CMR_{glu}. This suggests that these metabolic parameters may not be the primary indicators of extent or severity of brain damage. While CBF is crucial for maintaining the metabolic demands of brain tissue, the weak correlation indicates that other factors may play a more significant role in the pathophysiology of brain damage. It also emphasizes that CBF and CBV have a proportional relationship with each other during recovery. **(Marmarou et al., 2000)**

This may explain why prognosis of patients resuscitated from cardiac arrest still remains very poor despite the return of spontaneous circulation. The preservation of cerebral blood flow and volume alone is insufficient to prevent neurological damage if the underlying metabolic support, such as oxygen and glucose utilization, is compromised. One possibility is that the brain, in its compromised state, may be unable to effectively extract glucose from the blood, which can cause injury, despite the return of blood flow. **(Russo et al., 2018)** Another possibility is that low rates of blood flow in healthy brains may still contribute to brain injury. When blood

flow is restored after resuscitation, there is a brief period of cerebral hyperemia, where the blood-brain barrier can become more permeable leading to increased pressure and swelling. **(Bouma and Muizelaar, 1992)** This pressure can cause damage in vulnerable brain tissue, especially in regions of the brain that usually have lower rates of blood flow and volume.

Finally, it is also known that rapid restoration of blood flow often leads to better outcomes. **(Esdaille et al., 2020) (Olasveengen et al., 2020)** It may be that the length of time that blood flow was low or at zero during cardiac arrest is an important factor. This was not a measurement in this experiment and could help explain the amount and severity of reperfusion injury in a patient.

II. $CMRO_2$ and CMR_{glu} are More Correlated with Brain Injury Than CBF and CBV

Low ADC values tended to show stronger correlations with high $CMRO_2$ and CMR_{glu} values in healthy patients. This supports the idea that areas of the brain that have higher glucose and oxygen levels are more susceptible to injury. These regions, which are metabolically active, might be more vulnerable to damage due to their higher energy demands. When the regions are injured, the disruption in their metabolic processes is more pronounced, leading to the observed stronger correlations.

This finding underscores the importance of oxygen and glucose in maintaining brain integrity. It also highlights a potential target for post-resuscitation assessments, especially in patients with moderate to severe injury, where these correlations are the strongest. The strength of the correlations could also serve as a foundation to develop better predictive models for brain injury for early detection and intervention.

III. Patients with Minimal Injury (<1%) had Weak Correlations Between Brain Injury and Metabolism

When patients were clustered by their injury levels, correlations between their ADC values and each metabolism measurement tended to be weak and inconclusive. This trend continued even when correlations were separated between lesioned and non-lesioned regions of the brain suggesting that ADC values in minimally injured brains are not strongly linked to these metabolic parameters.

One explanation is that the cause of injuries in patients with minimal injury are more often a result of non-metabolic factors. These can include traumatic brain injuries during cardiac arrest or small-scale vascular bleeds. These non-metabolic factors can disrupt neural integrity and cause structural changes without significantly impacting the brain's metabolic processes, explaining the weak correlations.

IV. Patients with Moderate to Severe Injury (30-60%) had Stronger Correlations

The strongest positive and negative correlations were observed in the patients with moderate to severe injuries. In these regions, oxygen and glucose account for most of the stronger correlations, reinforcing the idea that metabolic processes play a significant role in the extent of brain injury. This suggests that further injury in the brain is closely linked to disruptions in oxygen and glucose utilization. This could be due to the heightened metabolic demands of these brain regions and their subsequent vulnerability to injury-related disruptions.

V. Correlations of Lesions with Metabolic Values is Region Dependent

It was revealed that correlation strength and direction could differ significantly between brain regions within a cluster. Although most of the regions of moderate to severely injured patients had strong negative correlations, some regions such as Brodmann Area 18 were consistently positive. These correlations indicate that injury in Brodmann Area 18 could be influenced by non-metabolic factors. Another explanation is that these regions are inherently more vulnerable to injury, regardless of their metabolic activity.

A broader region of interest includes the areas of the brain responsible for visual function, including BA8 which is responsible for rapid eye movements. These visual-related regions were among the most injured across clusters . This emphasizes that the strength of correlations with metabolic values can vary significantly based on specific functions and vulnerabilities of different brain areas. Regions involved in visual processing inherently have high metabolic demands due to their role in coordinating complex visual and motor functions. The high rate of injury in these suggests that they might be particularly susceptible to metabolic disruptions.

VI. Limitations

This thesis, while providing valuable insights into the relationship between brain injury and cerebral metabolic characteristics in post-cardiac arrest comatose patients, has several limitations that should be acknowledged. The study featured 83 patients, but after clustering by percentage of injury more than half of these patients were found to have less than 1% total brain injury. This diminishes the representation of other patients and limits the generalizability of the results. A larger sample size could eliminate any potential bias that may have affected correlation coefficients.

The correlations were conducted across two different datasets of patients: ADC MRIs from patients of UCSF-affiliated hospitals and neurologically normal patients from neuromaps. This may limit the ability to infer causality between metabolic changes and brain injury. The resting state metabolism of injured patients may be different than those of the metabolism map which may influence the strength and nature of observed correlations. This discrepancy may introduce variability and affect the accuracy of the conclusions drawn from this study.

Although the study included a regional analysis by clustering patients based on injury percentage, it did not account for other possible confounding variables such as patient demographic or cause of cardiac arrest. These factors can significantly influence both metabolic processes and brain injury outcomes, potentially affecting the strength and direction of the observed correlations. The absence of other factors also limits the ability to make causal conclusions about metabolism's effect on brain injury.

Acknowledging these limitations is crucial for making conclusions for the findings of this thesis. Future research should aim to address these limitations by increasing sample sizes, unifying datasets, and including potential confounding variables. Despite these limitations, this study provides a foundation for understanding the metabolic underpinnings of brain injury and highlights potential for personalized medicine approaches to improve patient outcomes.

VII. Conclusions and Future Work

This study highlights the complexity and regional dependency of the relationship between brain injury and metabolic values, such as CBF, CBV, $CMRO_2$, and CMR_{glu}. CBF and CBV showed weaker correlations with low ADC values compared to $CMRO_2$ and CMR_{glu}, suggesting that metabolic processes involving oxygen and glucose utilization are more closely

linked to the extent and severity of brain injury. This may help explain the poor prognosis of patients resuscitated from cardiac arrest despite the return of spontaneous circulation as the preservation of blood flow and volume alone is insufficient if metabolic support is compromised.

Regions with higher metabolic activity, particularly those involved in visual processing and rapid eye movements, such as BA18 and BA8, were among the most injured. This underscores the importance of these metabolic processes in maintaining brain integrity and also accents the vulnerability of some metabolically active regions to injuries.

Patients with minimal injury exhibited weak correlations between ADC values and metabolic measurements, likely due to the influence of non-metabolic factors such as traumatic brain injuries or small-scale vascular events. Conversely, patients with moderate to severe injuries displayed stronger correlations, emphasizing the critical role of oxygen and glucose metabolism in the progression of brain damage. It also demonstrates that prognosis and analysis regarding oxygen and glucose may be most effective on moderately to severely injured patients, instead of patients with minimal injuries.

With a clearer understanding of the relationship between these measurements of metabolism, future research could focus on integrating $CMRO_2$ and CMR_{glu} for prognosis to provide a comprehensive assessment of brain health. This would enhance the early detection of brain injuries and improve prognosis, especially in patients with moderate to severe injuries. Combining these assessments with clinical and neurological outcomes could serve as a foundation for clinical prediction models to aid neurologists in certain treatments.

The regional dependency of brain injury and metabolic correlations could also suggest the need for personalized treatment plans. Tailoring interventions to the specific metabolic and functional vulnerabilities of different brain regions can improve patient outcomes and recovery.

By integrating $CMRO_2$ and CMR_{glu} measurements, clinicians could assess the metabolic health of specific regions. Personalized metabolic profiles can reveal which areas are at greater risk of injury or are already compromised, before it becomes severe. This allows for proactive monitoring and early intervention to prevent injury progression.

Artificial Intelligence (AI) and predictive modeling can play a crucial role in enhancing the personalization of brain injury treatments. By analyzing large and complex datasets, AI algorithms can identify patterns and correlations not evident through traditional correlation analyses. It can also integrate various types of data including genetic information, clinical history, and patient demographics. Comprehensive metabolic profiles could be created accurately and quickly for physician review. Similarly, AI-powered predictive models can assess the risk of injury progression in each brain region, which could predict brain injury patterns and identify patients at higher risk of severe outcomes. In research, AI and predictive modeling can accelerate research by identifying biomarkers and targets associated with brain injury and metabolic dysfunction. These insights could inform the development of novel treatments and interventions. Collaborative research networks can share and analyze data from diverse patient populations, improving the generalizability and robustness of predictive models.

Bibliography

Albers, R. Wayne (Robert Wayne). “Basic Neurochemistry.” *(No Title)*. *cir.nii.ac.jp*, https://cir.nii.ac.jp/crid/1130282272953996800. Accessed 19 May 2024.

Bardt, Tillman F., et al. “Monitoring of Brain Tissue PO2 in Traumatic Brain Injury: Effect of Cerebral Hypoxia on Outcome.” *Intracranial Pressure and Neuromonitoring in Brain Injury*, edited by Anthony Marmarou et al., Springer, 1998, pp. 153–56. *Springer Link*, https://doi.org/10.1007/978-3-7091-6475-4_45.

Basu, Samar, et al. “Evidence for Time-Dependent Maximum Increase of Free Radical Damage and Eicosanoid Formation in the Brain as Related to Duration of Cardiac Arrest and Cardio-Pulmonary Resuscitation.” *Free Radical Research*, vol. 37, no. 3, Jan. 2003, pp. 251–56. *tandfonline.com (Atypon)*, https://doi.org/10.1080/1071576021000043058.

Björklund, Erik, et al. “Ischaemic Brain Damage after Cardiac Arrest and Induced Hypothermia–a Systematic Description of Selective Eosinophilic Neuronal Death. A Neuropathologic Study of 23 Patients.” *Resuscitation*, vol. 85, no. 4, Apr. 2014, pp. 527–32. *ScienceDirect*, https://doi.org/10.1016/j.resuscitation.2013.11.022.

Bouma, Gerrit, and J. Muizelaar. “Cerebral Blood Flow, Cerebral Blood Volume, and Cerebrovascular Reactivity after Severe Head Injury.” *Journal of Neurotrauma*, vol. 9 Suppl 1, Apr. 1992, pp. S333-48.

Brodmann, Korbinian. *Vergleichende Lokalisationslehre der Grosshirnrinde in ihren Prinzipien dargestellt auf Grund des Zellenbaues*. Barth, 1909.

Brooks, George A., and Neil A. Martin. “Cerebral Metabolism Following Traumatic Brain Injury: New Discoveries with Implications for Treatment.” *Frontiers in Neuroscience*, vol. 8, Feb. 2015. *Frontiers*, https://doi.org/10.3389/fnins.2014.00408.

Buckner, Randy L., et al. “The Organization of the Human Cerebellum Estimated by Intrinsic Functional Connectivity.” *Journal of Neurophysiology*, vol. 106, no. 5, Nov. 2011, pp. 2322–45. *journals.physiology.org (Atypon)*, https://doi.org/10.1152/jn.00339.2011.

Buunk, Gerba, et al. “Cerebral Blood Flow after Cardiac Arrest.” *The Netherlands Journal of Medicine*, vol. 57, no. 3, Sept. 2000, pp. 106–12. *ScienceDirect*, https://doi.org/10.1016/S0300-2977(00)00059-0.

Calabrese, E., et al. “Parieto-Occipital Injury on Diffusion MRI Correlates with Poor Neurologic Outcome Following Cardiac Arrest.” *AJNR. American Journal of Neuroradiology*, vol. 44, no. 3, Mar. 2023, pp. 254–60. *PubMed*, https://doi.org/10.3174/ajnr.A7779.

Chalkias, Athanasios, and Theodoros Xanthos. “Post-Cardiac Arrest Brain Injury: Pathophysiology and Treatment.” *Journal of the Neurological Sciences*, vol. 315, no. 1, Apr. 2012, pp. 1–8. *ScienceDirect*, https://doi.org/10.1016/j.jns.2011.12.007.

Chenevert, T. L., et al. “Diffusion Magnetic Resonance Imaging: An Early Surrogate Marker of Therapeutic Efficacy in Brain Tumors.” *Journal of the National Cancer Institute*, vol. 92, no. 24, Dec. 2000, pp. 2029–36. *PubMed*, https://doi.org/10.1093/jnci/92.24.2029.

Chugh, Sumeet S., et al. “Current Burden of Sudden Cardiac Death: Multiple Source Surveillance versus Retrospective Death Certificate-Based Review in a Large U.S.

Community." *Journal of the American College of Cardiology*, vol. 44, no. 6, Sept. 2004, pp. 1268–75. *ScienceDirect*, https://doi.org/10.1016/j.jacc.2004.06.029.

Cold, G. E. "The Relationship between Cerebral Metabolic Rate of Oxygen and Cerebral Blood Flow in the Acute Phase of Head Injury." *Acta Anaesthesiologica Scandinavica*, vol. 30, no. 6, 1986, pp. 453–57. *Wiley Online Library*, https://doi.org/10.1111/j.1399-6576.1986.tb02452.x.

Dienel, Gerald A. "Brain Glucose Metabolism: Integration of Energetics with Function." *Physiological Reviews*, vol. 99, no. 1, Jan. 2019, pp. 949–1045. *journals.physiology.org (Atypon)*, https://doi.org/10.1152/physrev.00062.2017.

Edgren, E., et al. "Assessment of Neurological Prognosis in Comatose Survivors of Cardiac Arrest." *The Lancet*, vol. 343, no. 8905, Apr. 1994, pp. 1055–59. *ScienceDirect*, https://doi.org/10.1016/S0140-6736(94)90179-1.

Esdaille, C. Jayson, et al. "Duration and Clinical Features of Cardiac Arrest Predict Early Severe Cerebral Edema." *Resuscitation*, vol. 153, Aug. 2020, pp. 111–18. *ScienceDirect*, https://doi.org/10.1016/j.resuscitation.2020.05.049.

Fiehler, Jens, et al. "Cerebral Blood Flow Predicts Lesion Growth in Acute Stroke Patients." *Stroke*, vol. 33, no. 10, Oct. 2002, pp. 2421–25. *ahajournals.org (Atypon)*, https://doi.org/10.1161/01.STR.0000032554.19600.60.

Glenn, Thomas C., et al. "Energy Dysfunction as a Predictor of Outcome after Moderate or Severe Head Injury: Indices of Oxygen, Glucose, and Lactate Metabolism." *Journal of Cerebral Blood Flow & Metabolism*, vol. 23, no. 10, Oct. 2003, pp. 1239–50. *SAGE Journals*, https://doi.org/10.1097/01.WCB.0000089833.23606.7F.

Hirsch, K. G., et al. "Multi-Center Study of Diffusion-Weighted Imaging in Coma After Cardiac Arrest." *Neurocritical Care*, vol. 24, no. 1, Feb. 2016, pp. 82–89. *PubMed*, https://doi.org/10.1007/s12028-015-0179-9.

Hirsch, Karen G., et al. "Prognostic Value of Diffusion-Weighted MRI for Post-Cardiac Arrest Coma." *Neurology*, vol. 94, no. 16, Apr. 2020, pp. e1684–92. *PubMed Central*, https://doi.org/10.1212/WNL.0000000000009289.

Iima, Mami, et al. "Apparent Diffusion Coefficient as an MR Imaging Biomarker of Low-Risk Ductal Carcinoma in Situ: A Pilot Study." *Radiology*, vol. 260, no. 2, Aug. 2011, pp. 364–72. *PubMed*, https://doi.org/10.1148/radiol.11101892.

Iordanova, Bistra, et al. "Alterations in Cerebral Blood Flow after Resuscitation from Cardiac Arrest." *Frontiers in Pediatrics*, vol. 5, Aug. 2017. *Frontiers*, https://doi.org/10.3389/fped.2017.00174.

Jørgensen, Martin Balslev, et al. "Postischemic Glucose Metabolism Is Modified in the Hippocampal CA1 Region Depleted of Excitatory Input or Pyramidal Cells." *Journal of Cerebral Blood Flow & Metabolism*, vol. 10, no. 2, Mar. 1990, pp. 243–51. *SAGE Journals*, https://doi.org/10.1038/jcbfm.1990.41.

Kelly, Daniel F., et al. "Cerebral Blood Flow as a Predictor of Outcome Following Traumatic Brain Injury." *Journal of Neurosurgery*, vol. 86, no. 4, Apr. 1997, pp. 633–41. *thejns.org*, https://doi.org/10.3171/jns.1997.86.4.0633.

Lancaster, Jack L., et al. "A Modality-Independent Approach to Spatial Normalization of Tomographic Images of the Human Brain." *Human Brain Mapping*, vol. 3, no. 3, 1995, pp. 209–23. *Wiley Online Library*, https://doi.org/10.1002/hbm.460030305.

Larsson, Elin, et al. “Stereological Assessment of Vulnerability of Immunocytochemically Identified Striatal and Hippocampal Neurons after Global Cerebral Ischemia in Rats.” *Brain Research*, vol. 913, no. 2, Sept. 2001, pp. 117–32. *ScienceDirect*, https://doi.org/10.1016/S0006-8993(01)02762-7.

Larsson, H. B., et al. “In Vivo Magnetic Resonance Diffusion Measurement in the Brain of Patients with Multiple Sclerosis.” *Magnetic Resonance Imaging*, vol. 10, no. 1, 1992, pp. 7–12. *PubMed*, https://doi.org/10.1016/0730-725x(92)90367-9.

Laver, Stephen, et al. “Mode of Death after Admission to an Intensive Care Unit Following Cardiac Arrest.” *Intensive Care Medicine*, vol. 30, no. 11, Nov. 2004, pp. 2126–28. *Springer Link*, https://doi.org/10.1007/s00134-004-2425-z.

Le Bihan, D., et al. “MR Imaging of Intravoxel Incoherent Motions: Application to Diffusion and Perfusion in Neurologic Disorders.” *Radiology*, vol. 161, no. 2, Nov. 1986, pp. 401–07. *PubMed*, https://doi.org/10.1148/radiology.161.2.3763909.

Markello, Ross D., et al. “Neuromaps: Structural and Functional Interpretation of Brain Maps.” *Nature Methods*, vol. 19, no. 11, Nov. 2022, pp. 1472–79. *www.nature.com*, https://doi.org/10.1038/s41592-022-01625-w.

Marmarou, Anthony, et al. “Contribution of Edema and Cerebral Blood Volume to Traumatic Brain Swelling in Head-Injured Patients.” *Journal of Neurosurgery*, vol. 93, no. 2, Aug. 2000, pp. 183–93. *thejns.org*, https://doi.org/10.3171/jns.2000.93.2.0183.

Mlynash, Michael, et al. “Temporal and Spatial Profile of Brain Diffusion-Weighted MRI After Cardiac Arrest.” *Stroke*, vol. 41, no. 8, Aug. 2010, pp. 1665–72. *ahajournals.org (Atypon)*, https://doi.org/10.1161/STROKEAHA.110.582452.

Moseley, M. E., et al. “Diffusion-Weighted MR Imaging of Acute Stroke: Correlation with T2-Weighted and Magnetic Susceptibility-Enhanced MR Imaging in Cats.” *AJNR. American Journal of Neuroradiology*, vol. 11, no. 3, May 1990, pp. 423–29.

Multimodal Surface Matching with Higher-Order Smoothness Constraints - ScienceDirect. https://www.sciencedirect.com/science/article/abs/pii/S1053811917308649?via%3Dihub. Accessed 19 May 2024.

Narotam, Pradeep K., et al. “Brain Tissue Oxygen Monitoring in Traumatic Brain Injury and Major Trauma: Outcome Analysis of a Brain Tissue Oxygen–Directed Therapy: Clinical Article.” *Journal of Neurosurgery*, vol. 111, no. 4, Oct. 2009, pp. 672–82. *thejns.org*, https://doi.org/10.3171/2009.4.JNS081150.

Neumar, Robert W., et al. “Post–Cardiac Arrest Syndrome.” *Circulation*, vol. 118, no. 23, Dec. 2008, pp. 2452–83. *ahajournals.org (Atypon)*, https://doi.org/10.1161/CIRCULATIONAHA.108.190652.

Nolan, Jerry P., et al. “Post-Cardiac Arrest Syndrome: Epidemiology, Pathophysiology, Treatment, and Prognostication: A Scientific Statement from the International Liaison Committee on Resuscitation; the American Heart Association Emergency Cardiovascular Care Committee; the Council on Cardiovascular Surgery and Anesthesia; the Council on Cardiopulmonary, Perioperative, and Critical Care; the Council on Clinical Cardiology; the Council on Stroke.” *Resuscitation*, vol. 79, no. 3, Dec. 2008, pp. 350–79. *ScienceDirect*, https://doi.org/10.1016/j.resuscitation.2008.09.017.

Olasveengen, Theresa M., et al. “Adult Basic Life Support: International Consensus on Cardiopulmonary Resuscitation and Emergency Cardiovascular Care Science With

Treatment Recommendations." *Resuscitation*, vol. 156, Nov. 2020, pp. A35–79. *ScienceDirect*, https://doi.org/10.1016/j.resuscitation.2020.09.010.

Regional Aerobic Glycolysis in the Human Brain | PNAS. https://www.pnas.org/doi/full/10.1073/pnas.1010459107. Accessed 19 May 2024.

Robinson, Emma C., et al. "MSM: A New Flexible Framework for Multimodal Surface Matching." *NeuroImage*, vol. 100, Oct. 2014, pp. 414–26. *ScienceDirect*, https://doi.org/10.1016/j.neuroimage.2014.05.069.

Russo, Juan J., et al. "Hyperglycaemia in Comatose Survivors of Out-of-Hospital Cardiac Arrest." *European Heart Journal. Acute Cardiovascular Care*, vol. 7, no. 5, Aug. 2018, pp. 442–49. *PubMed*, https://doi.org/10.1177/2048872616684685.

Sabedra, Alexa R., et al. "Neurocognitive Outcomes Following Successful Resuscitation from Cardiac Arrest." *Resuscitation*, vol. 90, May 2015, pp. 67–72. *ScienceDirect*, https://doi.org/10.1016/j.resuscitation.2015.02.023.

Safar, Peter. "Cerebral Resuscitation after Cardiac Arrest: Research Initiatives and Future Directions." *Annals of Emergency Medicine*, vol. 22, no. 2, Part 2, Feb. 1993, pp. 324–49. *ScienceDirect*, https://doi.org/10.1016/S0196-0644(05)80463-9.

Sotak, Christopher H. "Nuclear Magnetic Resonance (NMR) Measurement of the Apparent Diffusion Coefficient (ADC) of Tissue Water and Its Relationship to Cell Volume Changes in Pathological States." *Neurochemistry International*, vol. 45, no. 4, Sept. 2004, pp. 569–82. *PubMed*, https://doi.org/10.1016/j.neuint.2003.11.010.

Thijs, Vincent N., et al. "Clinical and Radiological Correlates of Reduced Cerebral Blood Flow Measured Using Magnetic Resonance Imaging." *Archives of Neurology*, vol. 59, no. 2, Feb. 2002, pp. 233–38. *Silverchair*, https://doi.org/10.1001/archneur.59.2.233.

Tiainen, Marjaana, et al. “Functional Outcome, Cognition and Quality of Life after out-of-Hospital Cardiac Arrest and Therapeutic Hypothermia: Data from a Randomized Controlled Trial.” *Scandinavian Journal of Trauma, Resuscitation and Emergency Medicine*, vol. 23, no. 1, Feb. 2015, p. 12. *Springer Link*, https://doi.org/10.1186/s13049-014-0084-9.

van den Brule, J. M. D., et al. “Cerebral Perfusion and Cerebral Autoregulation after Cardiac Arrest.” *BioMed Research International*, vol. 2018, May 2018, p. 4143636. *PubMed Central*, https://doi.org/10.1155/2018/4143636.

Wijman, Christine A.C., et al. “Prognostic Value of Brain Diffusion Weighted Imaging After Cardiac Arrest.” *Annals of Neurology*, vol. 65, no. 4, Apr. 2009, pp. 394–402. *PubMed Central*, https://doi.org/10.1002/ana.21632.

Wijman, Christine A. C., et al. “Prognostic Value of Brain Diffusion-Weighted Imaging after Cardiac Arrest.” *Annals of Neurology*, vol. 65, no. 4, 2009, pp. 394–402. *Wiley Online Library*, https://doi.org/10.1002/ana.21632.

Wu, Jianxiao, et al. “Accurate Nonlinear Mapping between MNI Volumetric and FreeSurfer Surface Coordinate Systems.” *Human Brain Mapping*, vol. 39, no. 9, 2018, pp. 3793–808. *Wiley Online Library*, https://doi.org/10.1002/hbm.24213.

Xu, Kui, et al. “Decreased Brainstem Function Following Cardiac Arrest and Resuscitation in Aged Rat.” *Brain Research*, vol. 1328, Apr. 2010, pp. 181–89. *ScienceDirect*, https://doi.org/10.1016/j.brainres.2010.02.080.

Yoon, Jung A., et al. “Quantitative Analysis of Early Apparent Diffusion Coefficient Values from MRIs for Predicting Neurological Prognosis in Survivors of Out-of-Hospital

Cardiac Arrest: An Observational Study." *Critical Care*, vol. 27, no. 1, Oct. 2023, p. 407. *Springer Link*, https://doi.org/10.1186/s13054-023-04696-z.

Appendix

Brodmann Area (Median % Injury)	Cluster 0 (minimal 0.1%)	Cluster 1 (moderate 15.0%)	Cluster 2 (severe 68.5%)	Cluster 3 (critical 96.4%)	Median of % of Injury in Region
Medial Wall	0.0%	0.0%	0.0%	0.4%	0.0%
???	0.6%	8.0%	52.0%	95.0%	30.0%
BA8	0.3%	12.4%	64.5%	99.1%	38.5%
BA6	1.3%	32.8%	84.4%	98.1%	58.6%
BA4	7.6%	55.4%	84.6%	98.7%	70.0%
BA9	0.1%	6.3%	51.7%	97.4%	29.0%
BA3	3.9%	47.0%	89.8%	99.4%	68.4%
BA1	4.1%	43.3%	87.5%	99.1%	65.4%
BA5	0.3%	35.9%	85.7%	99.8%	60.8%
BA7	0.3%	53.2%	93.5%	98.0%	73.4%
BA2	1.2%	46.9%	93.6%	98.2%	70.3%
BA31	0.1%	27.8%	83.8%	98.1%	55.8%
BA40	0.1%	21.6%	91.8%	92.8%	56.7%
BA44	0.2%	26.5%	84.8%	93.5%	55.6%
BA45	0.2%	12.9%	79.5%	97.6%	46.2%
BA23	0.1%	17.5%	61.6%	88.2%	39.5%
BA39	0.0%	56.3%	95.4%	96.2%	75.9%
BA43	0.2%	17.3%	81.8%	99.0%	49.6%
BA19	0.9%	65.5%	93.5%	95.9%	79.5%
BA47	0.0%	2.6%	60.3%	98.5%	31.5%

BA41	0.1%	31.4%	78.6%	96.3%	55.0%
BA30	0.0%	25.5%	64.8%	76.4%	45.1%
BA22	0.3%	35.0%	86.6%	95.0%	60.8%
BA42	0.2%	38.0%	88.7%	96.2%	63.4%
BA21	0.1%	15.7%	73.9%	96.8%	44.8%
BA38	0.3%	1.7%	10.6%	97.2%	6.2%
BA37	0.2%	51.0%	92.4%	95.1%	71.7%
BA20	0.2%	2.4%	25.9%	95.1%	14.1%
BA32	0.0%	0.7%	36.9%	96.8%	18.8%
BA24	0.1%	2.4%	41.4%	96.7%	21.9%
BA10	0.0%	0.6%	45.4%	98.4%	23.0%
BA25	0.0%	0.6%	4.4%	90.8%	2.5%
BA11	0.1%	1.2%	28.1%	97.2%	14.6%
BA46	0.1%	8.5%	80.3%	97.0%	44.4%
BA17	0.3%	51.3%	90.8%	96.0%	71.0%
BA18	1.1%	66.2%	94.7%	97.7%	80.4%
BA27	0.0%	0.0%	3.0%	84.4%	1.5%
BA36	0.2%	1.0%	0.9%	92.4%	0.9%
BA35	0.0%	0.9%	13.6%	91.4%	7.2%
BA28	0.0%	0.7%	0.9%	89.7%	0.8%
BA29	0.0%	0.0%	18.0%	82.8%	9.0%
BA26	0.0%	0.0%	20.0%	93.3%	10.0%
BA33	0.0%	0.0%	1.0%	95.8%	0.5%

Table A1. Summary of Median Injury Percentages of each Brodmann Area by Cluster: This table presents the median injury percentages for each Brodmann Area that, separated by each cluster. The ??? area is a subset of voxels that could not be attributed to a specific Brodmann region provided by the atlas.

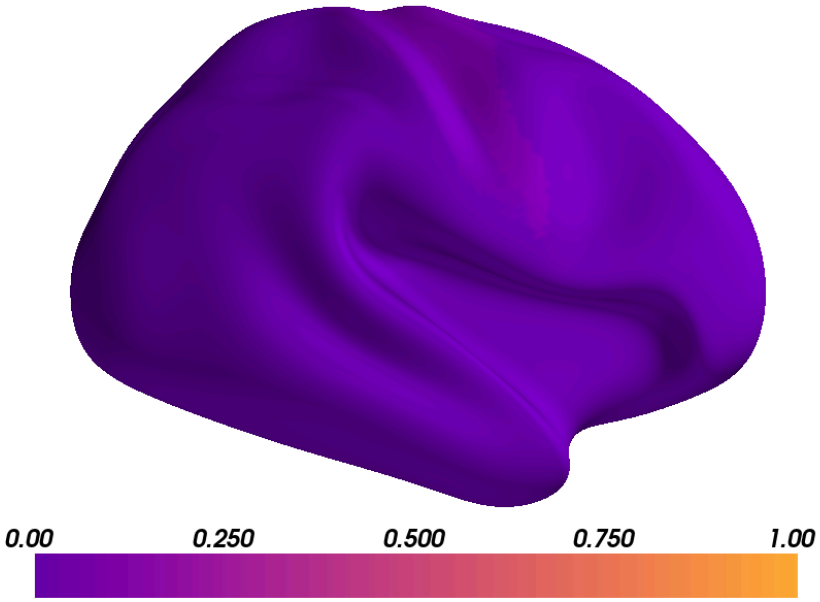

Figure A1. Injury Percentage across Minimal Cluster Brains: The median injury percentage across the brains in the minimal cluster for each Brodmann region are plotted on an inflated right hemisphere brain map.

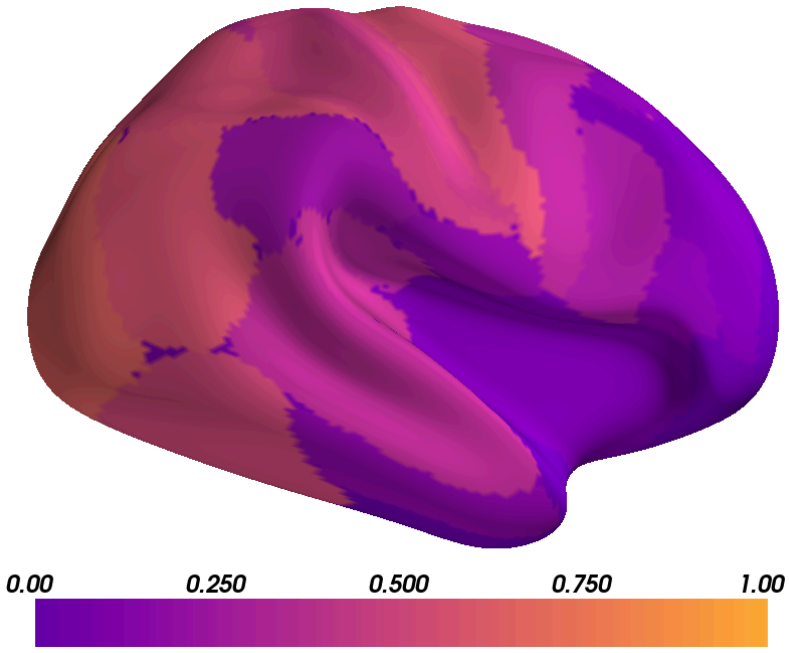

Figure A2. Injury Percentage across Moderate Cluster Brains: The median injury percentage across the brains in the moderate cluster for each Brodmann region are plotted on an inflated right hemisphere brain map.

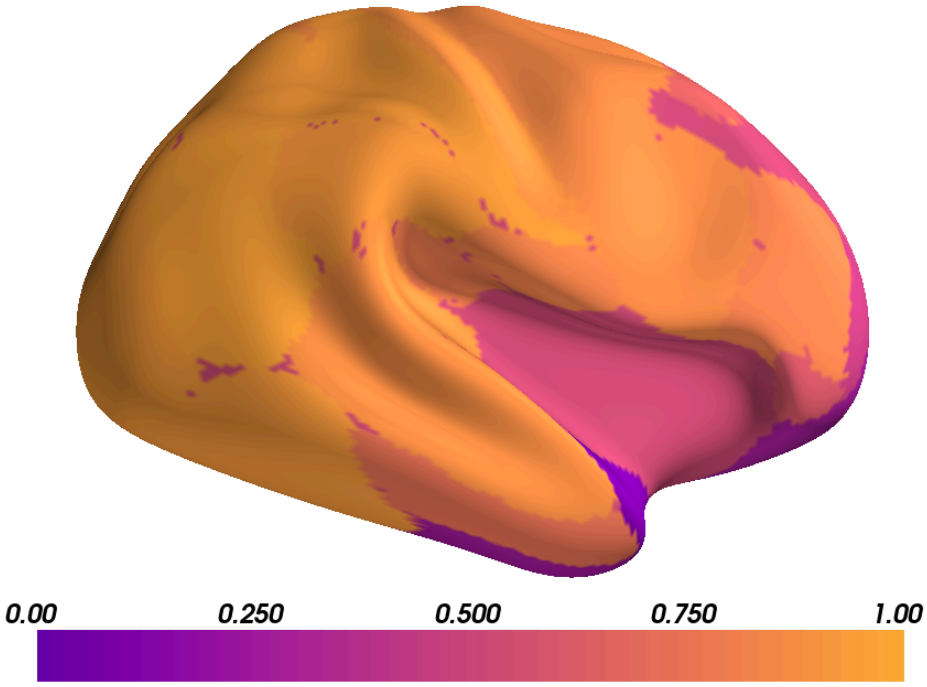

Figure A3. Injury Percentage across Severe Cluster Brains: The median injury percentage across the brains in the severe cluster for each Brodmann region are plotted on an inflated right hemisphere brain map.

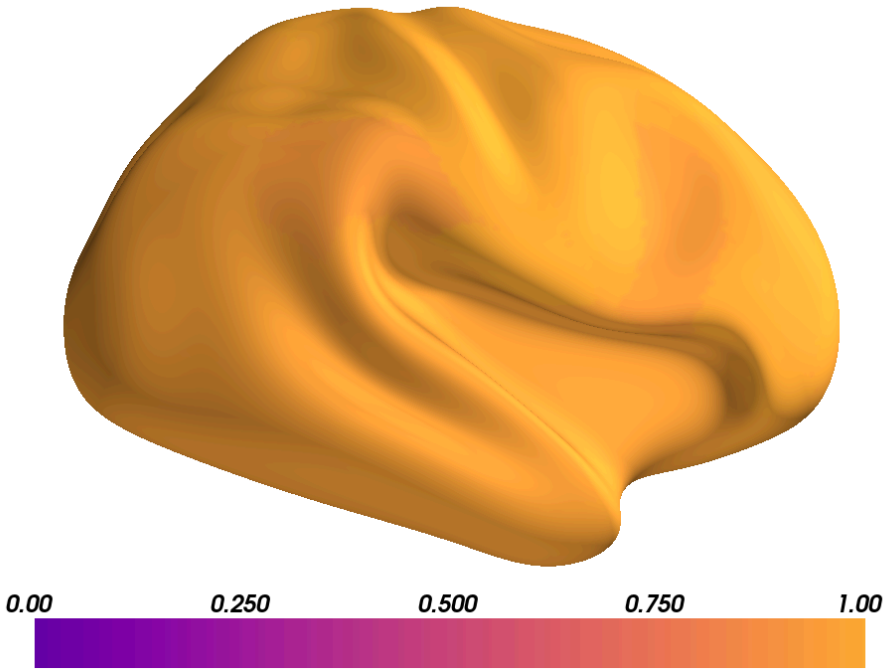

Figure A4. Injury Percentage across Critical Cluster Brains: The median injury percentage across the brains in the critical cluster for each Brodmann region are plotted on an inflated right hemisphere brain map.